Chinese Chemical Letters 32 (2021) 2117–2126

Contents lists available at ScienceDirect

Chinese Chemical Letters

journal homepage: www.elsevier.com/locate/cclet

Review

Current research progress of photopolymerized hydrogels in tissue engineering

Ao Sun, Xinye He, Xiao Ji, Danrong Hu, Meng Pan, Linghong Zhang, Zhiyong Qian*

State Key Laboratory of Biotherapy/Collaborative Innovation Center for Biotherapy, West China Hospital, West China Medical School, Sichuan University, Chengdu 610041, China

ARTICLE INFO

Article history:
Received 11 December 2020
Received in revised form 28 January 2021
Accepted 28 January 2021
Available online 2 February 2021

Keywords:
Hydrogels
Photopolymerization
Photoinitiators
Biofabrication
Tissue engineering

ABSTRACT

Owing to the special formation of photopolymerized hydrogels, they can effectively control the formation of hydrogels in space and time. Moreover, the photopolymerized hydrogels have mild formation conditions and biocompatibility; therefore, they can be widely used in tissue engineering. With the development and application of manufacturing technology, photopolymerized hydrogels can be widely used in cell encapsulation, scaffold materials, and other tissue engineering fields through more elaborate manufacturing methods. This review covers the types of photoinitiators, manufacturing technologies for photopolymerized hydrogels as well as the materials used, and a summary of the applications of photopolymerized hydrogels in tissue engineering.

1. Introduction

A hydrogel is a highly hydrophilic polymer crosslinking network. Hydrogels have high water content, good biocompatibility, and a very similar flexibility to that of tissue structure, making them excellent materials for tissue engineering [1–3]. The formation of hydrogels can be achieved through physical or chemical crosslinking [4,5]. Chemical crosslinking is the most commonly used crosslinking method, which is more stable than physical crosslinking and can improve the mechanical and degradation properties of hydrogel scaffolds in tissue engineering applications [6]. Chemical crosslinking includes Michael addition, Schiff base, enzymatic reaction, click chemistry, and photopolymerization. Photopolymerization has attracted much attention in the field of tissue engineering [7–11]. In recent decades, the application of hydrogels in tissue engineering has tended to have the characteristics of precise structure and flexible operation to control cell behavior, cell viability, and delivery of drugs. Photopolymerization has the advantages of flexible operation and spatiotemporal control of the formation of hydrogels, which can meet the needs of tissue engineering [12,13]. For example, the rapid reaction rate of photopolymerization can make the hydrogel easily encapsulated without obvious cell subsidence and maintain high cell viability [14]. The control of photopolymerization in the spatiotemporal formation of hydrogel can construct a complex crosslinking network [15], which is beneficial to control cell behavior and drug delivery [16]. In addition, photopolymerized hydrogels have mild reaction conditions (no need for high temperature and extreme pH conditions) and fluidity, which makes the use of the process less invasive and minimizes surgical trauma [17,18]. Moreover, photopolymerized hydrogels can accurately build custom-geometrically shaped biomaterials through 3D biological printing. It can produce structures that can reproduce the complex tissue and structure-function relationship existing in natural tissues and organs, so that implanted tissues can be repaired and loaded with drugs for delivery [19–21]. Therefore, in the field of tissue engineering, the application of photopolymerized hydrogels has a considerable potential [22–24]. In this review, we summarize the photoinitiators used in photopolymerized hydrogels, the materials currently used, the manufacturing technology of photopolymerized hydrogels, and the application of photopolymerized hydrogels in tissue engineering.

2. Photopolymerization

The principle of photopolymerization is to use light of appropriate wavelength to make the photoinitiators produce free radicals, ions or photoinduced step-growth polymerization, and then initiate polymerization with the monomer to form crosslinked hydrogels [25–28]. In this process, the intensity, concentration, and efficiency of the photoinitiators not only affect the reaction rate of photopolymerization, but also the biocompatibility

* Corresponding author.
E-mail addresses: anderson-qian@163.com, zhiyongqian@scu.edu.cn (Z. Qian).

https://doi.org/10.1016/j.cclet.2021.01.048

of the hydrogel is affected by the cytotoxicity and water solubility of the photoinitiators [29–31]. In addition, the materials used for photopolymerized hydrogels in tissue engineering require good biocompatibility, biodegradability, and functionality [32]. Meanwhile, the properties of the materials also affect the network structure and overall mechanical properties of hydrogels [33]. Therefore, choosing suitable photoinitiators and materials can reduce or avoid the impact of these problems on the practical application of tissue engineering.

2.1. Photoinitiators

Free radical photoinitiators are the most common photoinitiators in photopolymerization. Irradiation with an appropriate wavelength of light can decompose the photoinitiators to produce free radicals, thus initiating polymerization [34–37]. We have summarized the common photoinitiators (Table 1). Free radical photoinitiators are usually divided into two types: type I photoinitiators or type II photoinitiators. As shown in Fig. 1, type I photoinitiators decompose to produce free radicals after absorbing the appropriate wavelength of light [38]. As shown in Fig. 2, type II photoinitiators need to be combined with coinitiators to extract H-donor radicals and then initiate polymerization [39,40]. The most common type I photoinitiator is 2-hydroxy-4-(2-hydroxyethoxy)-2-methylpropiophenone (Irgacure 2959) [41,42]. It has been used for the encapsulation of photopolymerized hydrogels. Although there is p-hydroxyethoxy on Irgacure 2959, its hydrophilicity is not strong and its solubility is only 0.7% (w/v) [41]. Usually, it needs to

Table 1
Photoinitiators for photopolymerized hydrogels.

Photoinitiator	Chemical structure	λ_{abs} (nm)
Irgacure 2959	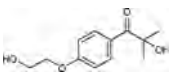	365
VA-086	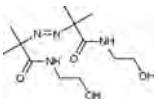	375
LAP	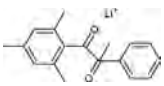	365, 405
2,3-bornanedione		470
Eosin Y	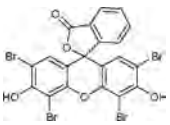	525
$Ru(Bpy)_3^{2+}$	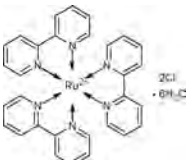	450

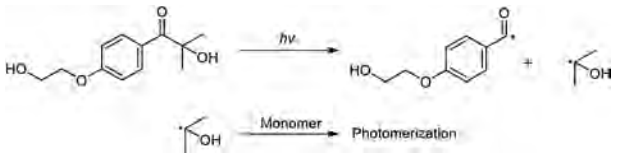

Fig. 1. Photopolymerization principle of a type I photoinitiator: For example, Irgacure 2959.

be heated or stirred sufficiently to dissolve. Irgacure 2959 was used for HepG2 cells encapsulated in methacrylated gelatin (GelMA), bone marrow mesenchymal stem cells (BMSCs) encapsulated in collagen-glycidyl methacrylate (Col-GMA)/methacrylated hyaluronic acid (HA-MA), human adipose mesenchymal stem cells (HADMSCs) encapsulated in GelMA/poly-ethylene glycol diacrylate (PEGDA3350)/alginate, and other cell-carrying hydrogels with high cell viability [43–45]. Irgacure 2959 has low cytotoxicity to cells, but its wavelength range is 200–370 nm. The wavelength of Irgacure 2959 for photopolymerization is 365 nm to avoid the mutagenicity of low wavelength ultraviolet light on cells and the oxidative stress produced by Irgacure 2959 [46,47]. However, the low polymerization efficiency of Irgacure 2959 at 365 nm will lead to an increase in initiation time, which requires the use of higher light intensity and higher initiator concentration, thus affecting the cell survival rate [48]. Although UVA1 damage radiation to cellular DNA, studies have shown that low-dose UVA1 radiation does not affect the gene expression of human mesenchymal stem cells [49]. The polymerization conditions, photoinitiator type and concentration will affect the cell survival. In addition, the ASTM standard cell line L929 could not accurately predict the viability of HMCS. It is also necessary to use relevant cells to evaluate the cell viability of photopolymerization hydrogel [50,51].

Another commonly used photoinitiator is 2,2-azobis [2-methyl-*n*-(2-hydroxyethyl) propionamide] (VA-086) [52]. Compared with Irgacure 2959, VA-086 has higher water solubility and lower cytotoxicity, and its absorption peak is at 375 nm. When used, VA-086 can be initiated by using lower wavelength ultraviolet light to avoid the mutagenicity of ultraviolet light on cells. Meanwhile, higher polymerization efficiency can reduce the light intensity and exposure time. VA-086 can be used to encapsulate HepG2 cells and bone marrow stromal cells in GelMA [43]. VA-086 can be used to encapsulate bovine chondrocytes in methacrylate-modified alginate and other loaded cell hydrogels [14,53,54]. However, the release of N2 gas from VA-086 induced by UV radicals may lead to an increase in the porosity of hydrogels [53,55].

The photoinitiator lithium phenyl-2,4,6-trimethylbenzoylphosphinate (LAP) was synthesized by Majima *et al.* [56]. Compared with Irgacure 2959, its water solubility is as high as 8.5% (w/v). LAP has a maximum absorbance at 365 nm and has a certain absorption in the visible range of 400–420 nm [57]. Therefore, LAP can be effectively photopolymerized in the visible light range, avoiding the mutagenicity of UV light on cells and the oxidative stress produced by it. Visible light has higher penetration than UV light [58]. Compared with Irgacure 2959, LAP has lower cytotoxicity and wider application conditions. For example, low-intensity LED lights can be used as portable and low-cost light sources. LAP can be used to encapsulate fibroblasts and mesenchymal stem cells

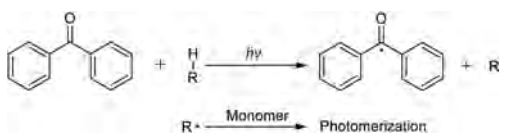

Fig. 2. Photopolymerization principle of a type II photoinitiator: For example, benzophenone/tertiary amine [39].

(MSc) in GelMA. LAP can be used to encapsulate human adipose-derived stem cells (hADSCs) in PEGDA and other cell-carrying hydrogels with high cell viability [57,59].

Camphorquinone (2,3-bornanedione) is widely used in type II photoinitiators [60]. Its absorption wavelength is between 400–500 nm, which can avoid the cytotoxicity of UV irradiation. Camphorquinone has good biocompatibility. It can be used to encapsulate human chondrocytes in methacrylate-functionalized carbamate, rabbit articular chondrocytes in styrene gelatin, and other cell-carrying hydrogels [61–63]. Compared with camphorquinone, another type II photoinitiator, Eosin Y (fluorescent dye), has higher water solubility and better biocompatibility [64]. It is widely used to encapsulate cells in GelMA. In addition, there are other type II photoinitiators, such as Bengal rose red and riboflavin, which have good biocompatibility compared with Eosin Y. Moreover, they can avoid the problem of overlapping, where the excitation and emission spectra of Eosin Y overlap with many fluorescent groups used in cell imaging [65,66].

Lim *et al*. constructed a new free radical photopolymerization system composed of ruthenium (Ru) and sodium persulfate (SPS) as water-soluble photoinitiators [29]. This photoinitiator can absorb photons in the visible light range to initiate light. When irradiated with visible light, Ru^{2+} is directly oxidized to Ru^{3+} and provides electrons to the SPS. After receiving electrons, SPS is decomposed into sulfate anions and sulfate radicals and then photopolymerized [67]. Ru/SPS is highly absorbable in the visible range, and its absorption peak is at 450 nm. Compared with other visible light initiators, such as LAP (the molar extinction coefficient (ε) at 405 nm is 30 L mol^{-1} cm^{-1}) and Eosin Y (at 525 nm, $\varepsilon \approx$ 100000 L mol^{-1} cm^{-1}), the ε of Ru/SPS at 450 nm is 14600 L mol^{-1} cm^{-1} [68]. In addition, Ru/SPS has less cytotoxicity. It showed higher viability and metabolic activity, which is used to encapsulate human articular chondrocytes in GelMA hydrogels. Ru/SPS will be a potential photoinitiator in the future.

2.2. Materials used in photopolymerized hydrogels

Hydrogels are highly hydrophilic polymer crosslinking networks. Their application in tissue engineering is first equipped with a highly hydrated environment (water content greater than 90%) to fit the water environment *in vivo*. Therefore, the photopolymer materials needed are water-soluble polymers [69–73]. To encapsulate cells and avoid the effects of photopolymerization and degradation on cells, the photopolymer materials used need to be biocompatible in a series of reaction processes [74]. In addition, the photopolymer materials used in tissue engineering need to have certain biological activities, which can adapt to the physiological environment of cells and the functions of supporting cells in the repair process (such as proliferation, differentiation, adhesion, and migration.) and certain biodegradability [75–77].

Natural materials are the main components of photopolymerized hydrogels used in tissue engineering. The natural materials usually have better biocompatibility and biodegradability than synthetic materials. In addition, many natural materials are the main components of the extracellular matrix (ECM) or can imitate the characteristics of the ECM [78–81]. Gelatin is the hydrolyzate of collagen, which has an amino acid composition similar to collagen and has no immunogenicity [82,83]. It is one of the most common natural materials used in tissue engineering. Gelatin retains the natural cell-binding motifs (tripeptide Arg-Gly-Asp (RGD)), which can effectively promote cell adhesion and diffusion along with the matrix and has matrix metalloproteinase (MMP)-sensitive degradation sites [84]. Owing to the poor mechanical properties of gelatin, the problem can be effectively improved using photopolymerization after chemical modification. The target functional group is introduced by modifying the lysine unit or glutamic acid/aspartate unit on gelatin [85] and then Irgacure 2959 is used for photopolymerization. GelMA has been used in many tissue engineering hydrogels (Fig. 3) [86]. Gelatin can also form hydrogels through the photopolymerization of thiol-ene. Divinyl adipate (DVA) is used to modify gelatin to obtain vinyl ester gelatin [87,88]. The vinyl ester gelatin hydrogel showed low cytotoxicity. Gelatin can also be modified by allyl glycidyl ether to obtain allyl gelatin (Gelage). Gelage can be photopolymerized by a thiol-ene reaction. The mercaptan in photopolymerization can be provided by reducing *N,O*-bis(trimethylsilyl)acetamide, 4-Arm PEG thiol, l-dithiothreitol, and other multifunctional thiol crosslinking agents [85,86]. At the same time, multifunctional thiol crosslinking agents can also enhance the mechanical properties of gelatin.

HA is a linear polysaccharide composed of D-glucuronic acid and DN acetylglucosamine as repeating units, which is ubiquitous in almost all connective tissues [89,90]. As a component of ECM, HA has natural biocompatibility and plays an important role in regulating many cell behaviors and tissue functions, including cell migration, proliferation, differentiation and angiogenesis. Therefore, HA is widely used in tissue engineering, and chemical modification can effectively regulate the mechanical properties of HA hydrogels [90]. For example, HA can be modified by methacrylic anhydride to obtain HA-MA (Fig. 4) and then polymerized by an Irgacure 2959 photoinitiator to make the hydrogel degrade more slowly [91]. HA was also modified with glycidyl methacrylate to obtain HA-GMA, and then to enhance its mechanical properties by photopolymerization [92]. Qin *et al*. synthesized HA-VE using lipase-catalyzed transesterification between HA and DVA [93]. Compared with HA-MA, HA-VE has lower toxicity and higher photocatalytic activity. In addition, HA-VE can also form hydrogels through the photopolymerization of thiol-ene to improve its reactivity.

Silk fibroin is a protein polymer extracted from Bombyx mori, which is linked by disulfide bonds. Silk fibroin is mainly composed of amino acids, such as glycine, alanine, and serine. It has been used as a biomedical suture for decades [94,95]. It has good mechanical properties, good biocompatibility, and promotes cell adhesion, and is widely used in cartilage and bone repair. In the past, the preparation of silk fibroin hydrogel had problems such as slow gelation, the influence of the preparation process on cell viability, and uneven structure [96]. The preparation of silk fibroin hydrogels through photopolymerization can effectively overcome these problems. As shown in Fig. 5, the common modification method is to use glycidyl methacrylate and silk fibroin to prepare Sil-GMA in lithium bromide solution at 60 °C [96,97]. In addition, 2-isocyanatoethyl methacrylate can be used to react with silk fibroin to produce methacrylated silk fibroin. Methacrylic anhydride can also be used to produce methacryloyl silk protein [98]. Recently, Whittaker *et al*. used a Ru/SPS photoinitiator system for rapid photopolymerization to prepare high-elastic silk fibroin [99]. Natural materials for photopolymerization also include polyglutamic acid, chitosan, sodium alginate, and fibrin [100–102]. These natural materials usually have the advantages of biocompatibility, promoting cell adhesion, and antibacterial activity. They can be modified to prepare biocompatible and biodegradable photopolymerized hydrogels; therefore, they have great application value in tissue engineering [103].

Compared with natural materials, synthetic materials have the characteristics of easy preparation, low cost, a biological blank state, and no immunogenicity. Moreover, synthetic materials have the advantages of batch uniformity and reproducible control at the molecular level (*e.g.*, composition, degradability, and hydrogel conformation) [104,105]. They can be functionalized and have more diverse applications. For example, polyethylene glycol (PEG) is a synthetic polymer with excellent hydrophilicity, biocompatibility, and negligible immunogenicity [106]. It is widely used in cell

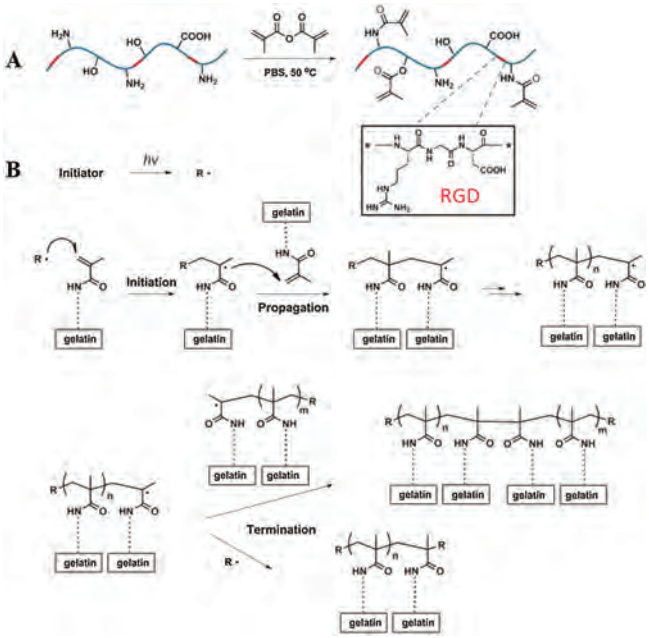

Fig. 3. Preparation of photopolymerization of GelMA hydrogels. (A) The gelatin was methacrylated using methacrylic anhydride. (B) The free radical initiating reaction of the GelMA photopolymer. Reproduced with permission [86]. Copyright 2015, Elsevier.

encapsulation, hydrogel scaffolds, drug delivery, and other fields. Photopolymerization can effectively control the mechanical properties, geometry, and size of PEG hydrogel, thus affecting cell activity and drug delivery [107–109]. At present, the common modification method involves the reaction of the hydroxyl side group of PEG with acryloyl chloride/methacryloyl chloride to obtain poly (ethylene glycol) diacrylate (PEGDA)/poly(ethylene glycol) dimethacrylate (PEGDMA) [110]. Sawhney *et al.* constructed a biodegradable PEG photopolymer hydrogel. The oligomers containing α-hydroxy acid were introduced into the PEG chain segment, and the degradation rate was controlled by controlling the amount of α-hydroxy acid and crosslinking degree [111]. In addition, Qin *et al.* synthesized PEG-based vinyl ester (PEGDVE) [112]. Compared with PEGDA, it has less irritation and avoids the cytotoxicity of unreacted acrylate groups. The results show that PEGDVE has less cytotoxicity than PEGDA/PEGDMA and can be photopolymerized by the thiol-ene method.

Polyvinyl alcohol (PVA) is a synthetic material with excellent biocompatibility and good mechanical properties (viscoelasticity), which has been approved by the FDA. PVA has been widely studied and applied in a variety of soft tissue engineering (such as artificial articular cartilage) implants and cardiovascular tissue [113]. At present, the modification method of PVA involves the reaction of the hydroxyl group of PVA with GMA under the catalysis of 4-dimethylaminopyridine (DMAP) to prepare methacrylated PVA (PVA-MA) [114]. Moreover, PVA can also react with methacrylic anhydride to form PVA-MA [115]. In addition, the phenyl azide group can also be introduced into PVA to synthesize photoreactive PVA (PRPVA) [116].

Unmodified synthetic materials usually lack certain biological activity. For example, compared with other natural polymers, PVA lacks certain cell adhesion and functional biological recognition sites [114]. In addition, the ability of these hydrogels to support cell differentiation is also limited. Therefore, synthetic materials can be functionalized (such as modified RGD and fibronectin) and combined with natural polymer materials (such as gelatin and alginate) to form bioactive composite hydrogels [117–120].

3. 3D printing application of photopolymerized hydrogel

In the application of hydrogels in tissue engineering, it is important to simulate highly controlled ECM structures [121]. The properties of the hydrogel matrix, including the mechanical properties, geometry, and size of the sieve, affect the proliferation, migration, differentiation, tissue regeneration, transportation, and nutrient exchange of different macromolecules [122,123]. Therefore, constructing a complex structure of hydrogel to simulate the complexity of the microenvironment *in vivo* can provide better tissue-specific biological functions. Photopolymerization can effectively control the formation of hydrogels in space and time accurately. It is possible to construct complex hydrogels with high resolution and precision using photopolymerization additive manufacturing technology [124,125]. The following will introduce several types of commonly used photopolymerization additive manufacturing technology.

3.1. Micropatterning

Micropatterning is a simple and convenient operation technology, and its hydrogel structure can be micron-sized. The use of micropatterning technology to produce hydrogels requires the initiation of light sources, photomasks, and hydrogel precursors containing initiators [126,127]. First, a photomask containing a required pattern is needed. Then, under light irradiation, the hydrogel precursors of the transparent part of the photomask are polymerized to form the desired pattern and wash the remaining unpolymerized part [128]. Tsang *et al.* used three different photomasks to carry out multi-layer photopolymerization of PEGDA containing different chemicals, and then embedded hepatocytes into complex structured hydrogels to form liver tissue constructs (Fig. 6) [129]. They controlled the height of the structure by moving the gasket and constructed a hydrogel with a multi-layered and complex structure. Compared with the cells without micropatterning, these cells remained alive after manufacturing and showed higher albumin and urea excretion.

3.2. Stereolithography (SLA)

SLA technology was developed in the 1980s [130]. It works in a container equipped with a gel front fluid. The laser light source photopolymerizes the gel on the manufacturing platform moving on the vertical plane according to the set instructions and moved by the X and Y axes. When all the points on one layer are crosslinked, the focal plane changes and creates the next layer (Fig. 7). This method is used to fabricate complex 3D structures with high resolution. Because the entire area should be scanned for each focal plane, the SLA can transfer the CAD model into a 3D

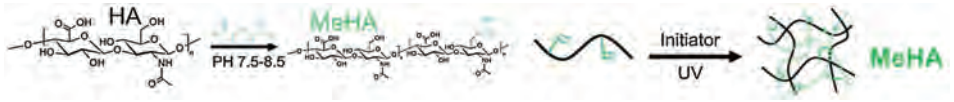

Fig. 4. Modified hyaluronic acid (HA): Methacrylated HA (MeHA) for photopolymerization. Methacrylic anhydride was used to methacrylate HA. Reproduced with permission [91]. Copyright 2016, American Chemical Society.

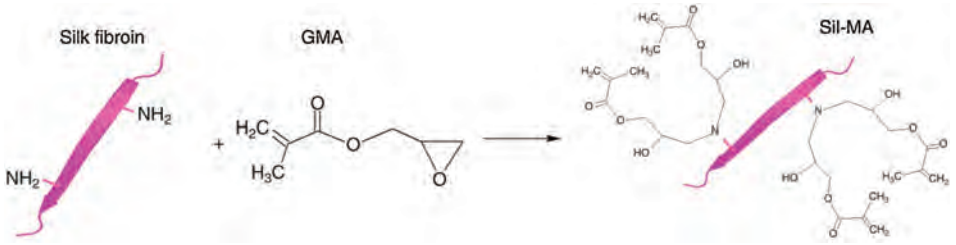

Fig. 5. Modified silk fibroin (SF): Methacrylic anhydride was used to methacrylate SF. Reproduced with permission [97]. Copyright 2018, Springer Nature.

structure accurately. It has great application in the fabrication of tissue engineering scaffolds and *in vitro* tissue models [131]. Lara *et al.* constructed a 3D printing hydrogel scaffold based on GelMA/PCL-MA using stereolithography technology [132]. The objective was to construct an acellular tissue scaffold mimicking the structure of physiological intestinal villi. Chen *et al.* constructed a 3D printing ECM/GelMA/exosome scaffold with a radial channel using SLA, which was used to treat osteochondral defect regeneration [133]. Melissinaki *et al.* constructed a PLGA based scaffold for neural tissue engineering through SLA. This scaffold has good biocompatibility and can make neuroblastoma cells proliferate [134]. Compared with micropatterning, SLA has a lower cost, shorter consumption time, and higher automation and resolution in the manufacturing of large structures.

3.3. Digital optical processing (DLP)

Compared with the point-to-point exposure polymerization of SLA, DLP can use a digital mask and light source to polymerize the whole layer in a single exposure. In a DLP system, the photon source illuminates from the bottom of the resin bath, and the building platform is dipped into the resin from above [135]. Therefore, DLP can achieve 3D manufacturing by consuming a small amount of resin. Hong *et al.* constructed a silk-GMA hydrogel scaffold containing chondrocytes using DLP [136]. It can effectively promote the proliferation and differentiation of chondrocytes *in vitro*, and a new cartilage tissue was observed *in vivo* (Fig. 8). Hong *et al.* developed an acrylic hyperbranched glycerol (AHPG) cross-linking agent that can control the drug release rate and the variable mechanical microenvironment of hydrogels [137]. DLP was used to print biological inks containing APHG to generate cell-loaded microgels of various shapes and sizes for tissue engineering applications. Compared with SLA, DLP has a higher printing speed, makes the hydrogel structure more uniform, and provides higher cell viability, thus reducing the damage to cells and making rapid production.

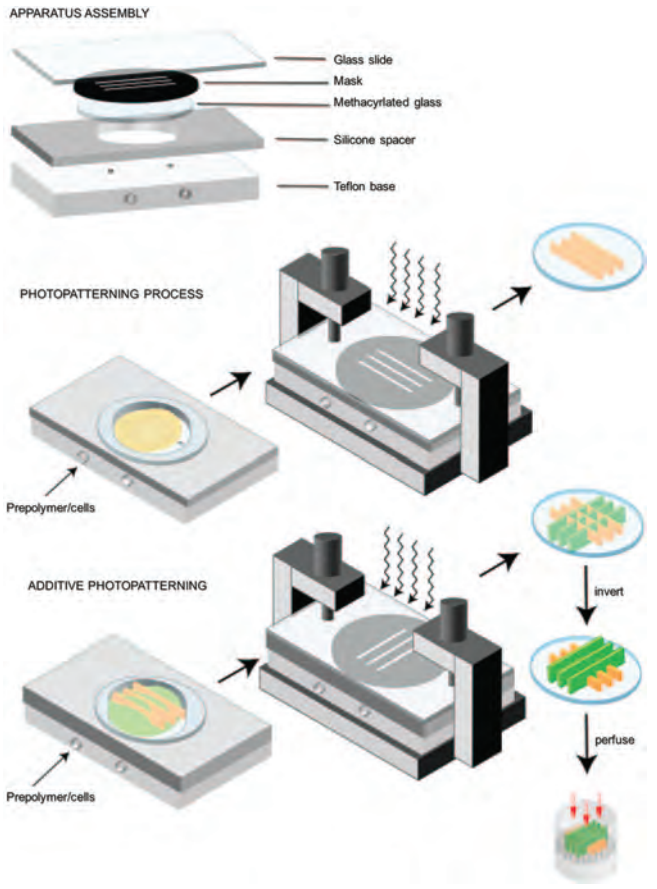

Fig. 6. Fabrication of cellular hydrogels using photomask-based additive photopatterning. The photomask and the cell-filled hydrogel precursors are shown in schematic form. Copied with permission [129]. Copyright 2006, John Wiley and Sons.

4. Application in tissue engineering

4.1. Application in skin wound

The skin is the largest organ of the human body and the last obstacle between the human body and the external environment. Skin damage caused by physical and chemical factors, such as trauma, burn, surgical incision, and infection, has become a serious clinical problem, affecting millions of patients worldwide [138,139]. Hydrogels are widely used in skin wound healing in tissue engineering owing to their biocompatibility, hydration, flexibility, and versatile characteristics. Skin wound healing is a complex biological cascade process, which requires the interaction of cell matrix, dermal and epidermal cells, the release of cytokines, the generation of mesenchymal cells, and capillaries to replace and regenerate the lost skin tissue [140,141]. The photopolymerized hydrogel exhibits good fluidity. It can encapsulate the drug *in situ* and quickly fill the irregular wound site. Moreover, photopolymerized hydrogels can be used at physiological pH and room temperature to encapsulate cells to maintain high cell viability. It is an ideal method for skin wound healing [142].

For example, Gozde *et al.* loaded adipose-derived stem cells (ADSCs) into a bioink composed of GelMA and HAMA to construct a dermal substitute through photopolymerization [143]. The hydrogel exhibited good transparency with 85% transmittance and allowed observation of the complete visual field of the wound site. The results showed that the hydrogel had good porosity and provided a suitable microenvironment for the proliferation of ADSCs. Confocal microscopy showed that the hydrogel demonstrated a large amount of angiogenesis in the chicken aortic arch assay and chicken chorionic villi (CAM) assay. This indicates that the ADSC/GelMA/HAMA hydrogel shows regeneration and angiogenesis. Skardal *et al.* used a thiol-ene reaction to prepare heparin-

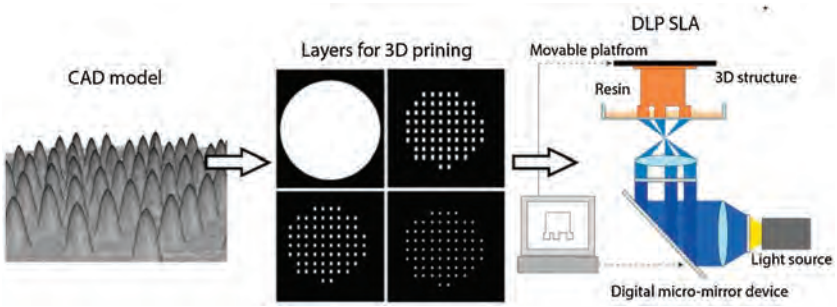

Fig. 7. SLA printing process for converting the CAD model into a 3D structure. The laser source photopolymerized the gel on the manufacturing platform according to the instruction, and the hydrogel is printed layer by layer. Reproduced with permission [132]. Copyright 2020, Elsevier.

conjugated hyaluronic acid (HA-HP) as a carrier for cell delivery, loading amniotic fluid-derived stem cells (AFS) (Fig. 9) [144]. The hydrogel was coated on the wounds of rats using biological printing. The results showed that the hydrogel could release the total protein, FGF, and VEGF secreted by AFS. At the same time, HA-HP is easily degraded *in situ*, which makes it easier for the cells to remodel during the healing process. In animal experiments, the hydrogel could accelerate the closure of full-thickness wounds in mice, induce an increase in angiogenesis, and lead to the formation of ECM.

4.2. Application in dentistry

In dentistry, photopolymerization is a traditional method for the rapid solidification of dental restorative materials. Most of them are composed of bisphenol-A-glycidyl methacrylate (Bis-GMA), urethane dimethacrylate (UDMA), triethyleneglycol dimethacrylate (TEGDMA), and other monomers [145–147]. It is difficult to use them in dental regeneration because of the lack of biocompatibility and the cytotoxicity of monomers. Photopolymerized hydrogels composed of gelatin, HA, PEG, and other materials can be used for cell encapsulation with biocompatibility. They can also control and regulate mechanical properties, swelling rate, and degradation rate, which has been widely used in dental regeneration [148–150]. For instance, Monteiro *et al.* constructed a dental curing light (DL) to encapsulate odontoblast-like cells (OD21) into GelMA and photopolymerized with LAP (Fig. 10) [151]. GelMA hydrogels showed higher cell viability. Fukaya *et al.* used poly(*N,N*-dimethylaminopropylacrylamide) as the photoinitiator and the derivatization of eosin to gelatin as a material to construct

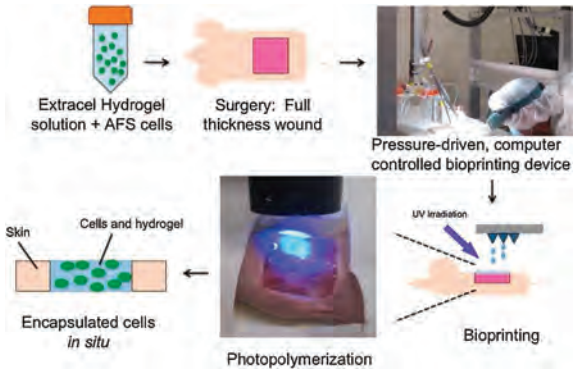

Fig. 9. The photopolymerized hydrogel can quickly encapsulate cells, and can quickly fill skin wounds after exposure to light. Copied with permission [144]. Copyright 2016, John Wiley and Sons.

gelatin (eosin-gelatin) [152]. This hydrogel showed better biocompatibility for mouse vascular endothelial cells (ECs). Compared with the control group, the hydrogel could effectively promote the proliferation of ECs and showed good periodontal regeneration ability. Bae *et al.* loaded GDF-5 onto ZrO_2 coated with HA hydrogel and used Irgacure 2959 for photopolymerization to obtain osteogenic materials [153]. This osteogenic material can control the release of GDF-5 and promote the proliferation and differentiation of MG63 cells, which can be used in dental osseointegration.

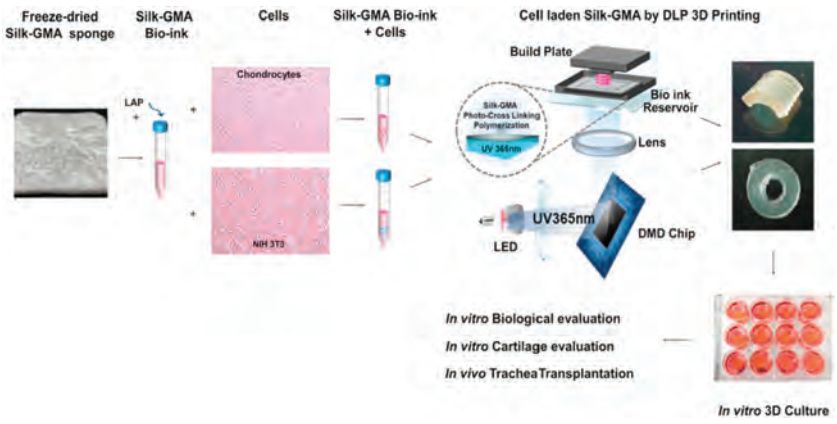

Fig. 8. Schematics of DLP bioprinting using Sil-GMA and chondrocytes. The cells are loaded into the hydrogel precursors of Sil-GMA. The photon source illuminates the hydrogel precursors from the bottom of the platform to construct the Sil-GMA hydrogel. Reproduced with permission [136]. Copyright 2020, Elsevier.

4.3. Application in bone tissue

The musculoskeletal system is the structural framework of the human body, providing physical support. Many factors can lead to bone tissue damage, therefore, there is an important clinical demand for functional bone tissue manufacturing [154,155]. Photopolymerized hydrogels can rapidly fill in clinical operations and effectively adjust and construct the microenvironment of surrounding tissues. It has great advantages in bone tissue repair. Zhai *et al*. prepared a PEG-laponite scaffold through the photopolymerization of PEGDA and nanocomposites (laponite) with the photoinitiator 2-hydroxy-2-methyl-1-phenyl-1-propanone (Irgacure 1173) (Fig. 11) [156]. HA fibers loaded with osteoblasts were further extruded between each PEG-laponite to be used in bone repair. The experimental results showed rapid bone growth and good integration with exogenous cells in ectopic osteoinduction experiments. Cidonio *et al*. combined laponite with GelMA to obtain a scaffold with high mechanical strength (range of 0.4–3.5 MPa) and high water content (72%–83.5%) using photopolymerization [157]. The rat model of tibial defect showed a good effect on bone regeneration.

Because hydrogels have excellent biocompatibility and high water content, similar to the extracellular matrix of cartilage, which can transfer load from the environment to chondrocytes, it has considerable potential in cartilage tissue repair [158]. In addition, photopolymerized hydrogels have the advantages of injectable and mild reaction conditions, which can fill irregularly shaped cartilage damage and maintain high cell viability. It has great advantages in cartilage regeneration. For example, Shao *et al*. prepared maleic-functionalized chitosan (MCh) and methacrylic esterified silk fibroin (SF) using photopolymerization to prepare MCh in MSFNP hydrogels loaded with TGF-beta [159]. The results showed that the hydrogels had good biocompatibility with human bone marrow-derived mesenchymal stem cells (BMDSCs) and promoted cell proliferation and adhesion, which could be used in cartilage tissue regeneration. Lin *et al*. used a methacrylic acid gelatin (mGL)-based hydrogel to encapsulate human bone marrow mesenchymal stem cells (hBMSC) and then used visible light photopolymerization [160]. The results showed that hydrogels had excellent mechanical properties and could effectively integrate with natural cartilage tissue after implantation. In addition, hBMSCs showed good growth and TGF-β3-induced chondrogenesis.

4.4. Application in the cardiovascular system

The cardiovascular system consists of the heart and peripheral circulation, which ensures the exchange of nutrients, waste, and gas as well as the transport of hormones, immune system components, and other molecules in the body [161]. Owing to the limited regenerative capacity of the myocardium, the heart is unable to recover from functional myocardial cell damage. The aim of cardiac tissue engineering is to implant cells to restore vascular transport and myocardial function. Because of the structural complexity of the heart, the function of the heart cannot be maintained only by the diffusion of nutrients from the inside to outside of the hydrogel and simple cell encapsulation [162,163]. Photopolymerized hydrogels can be widely used in the repair of heart tissue because they can construct and simulate the complex structure of the microenvironment *in vivo*.

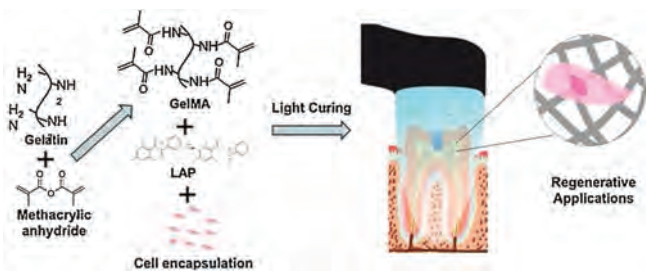

Fig. 10. Schematic of photopolymerization of GelMA hydrogel for regenerative endodontic treatment. The cells are loaded into the GelMA hydrogel precursor and filled into the pulp root canal. Reproduced with permission [151]. Copyright 2018, Elsevier.

For example, Shweta Anil Kumar *et al*. used bioink containing fibrin and furfural-gelatin (gel-fu) to fabricate scaffolds through visible light polymerization for culturing cardiomyocytes (CM) and cardiac fibroblasts (CF) [164]. They used CAD software to control and extrude the way to print and build a herringbone pattern to induce cell arrangement and growth (Fig. 12). The results showed that the scaffold could improve the cell arrangement and support the cardiac-specific function of the embedded cells. It can form heterogeneous cell coupling between CM and CF, to imitate the applicability of the cardiac tissue. Mohammad *et al*. used alginate doped with carboxyl-functionalized carbon nanotubes (CNTs) and methacrylated collagen (mecol) to produce heart patches [165]. Human coronary artery endothelial cells (HCAECs) were encapsulated in bioink and micropatterned using UV light. The height and thickness of the microchannels in the heart patch were 400 μm and 300 μm, respectively. The results showed that the cells were evenly distributed along the patterned chain, and incorporation of CNTs into the alginate matrix significantly improved the mechanical properties and electrical conductivity of the cardiac patch and enhanced cell adhesion and elongation. Hybrid implants promoted HCAEC proliferation, migration, and differentiation, represented by the lumen-like formation in the implant within 7–10 days *in vitro*.

5. Summary and outlook

Photopolymerization can effectively control the formation of hydrogels from time and space, and its mild reaction conditions enable it to be used in most tissue engineering applications. The advantages of photopolymerized hydrogels in constructing complex structures, encapsulating cells, and delivering drugs have considerable potential in tissue engineering. This paper briefly summarizes the principle of photopolymerization, including photoinitiators, materials, and manufacturing methods for photopolymerized hydrogels. The choice of photoinitiators, materials, and manufacturing technology is very important for the construction of photopolymerized hydrogels. They not only affect the physical and chemical properties of hydrogels, such as structure, mechanical properties, and degradation but also have a great influence on cell activity and cell-specific function. Flexible selection and application can better make the hydrogel simulate the microenvironment of the body, ensure the exchange of nutrients, and the proliferation, differentiation, and migration of cells.

With the development of computer simulation and various biological processing technologies, the future development direction of photopolymerized hydrogels will provide higher resolution, accuracy, and flexibility to reconstruct the structure of complex tissues and structure functional relationships existing in natural tissues and organs, to meet the needs of different clinical applications [166,167]. The new four-dimensional (4D) printing can break through the limitation of static printing and realize 4D printing, which can change the structure dynamically and respond to the environment [168,169]. Hydrogel changes the shape, characteristics, and function of the printing structure according to the simulation, forming a variety of cell types with hierarchical structures to better simulate the tissues and organs in the body. Gou *et al*. constructed a noninvasive 3D printing technology, using

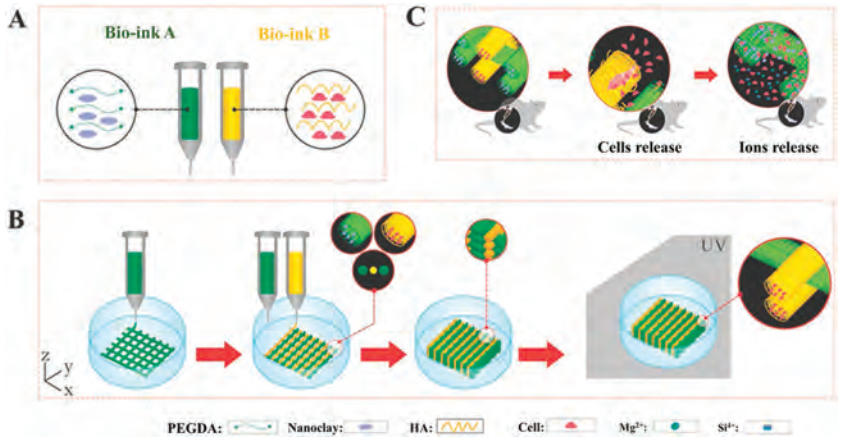

Fig. 11. Schematic of photopolymerized hydrogel 3D printing in tibial restoration. (A) The composition of bioink. (B) The 3D-bioprinting process of the hydrogel. (C) Schematic of tibia repair experiment. Reproduced with permission [156]. Copyright 2017, John Wiley and Sons.

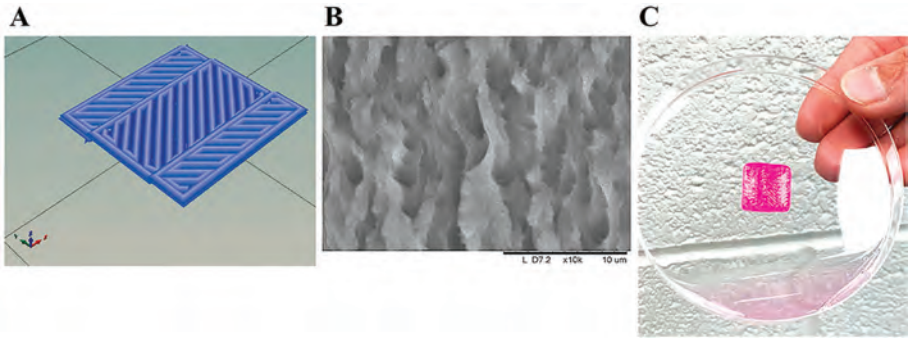

Fig. 12. Herringbone construct casted with the scaffolds. (A) CAD of a 3D printed pattern. (B) SEM of a characteristic 3D printed pattern. (C) Image of a 3D printed square pattern fabricated using the fibrin-gelatin bioink. Copied with permission [164]. Copyright 2019, American Chemical Society.

a digital near-infrared photopolymerization (DNP) process to locally inject biological inks into photopolymerization layer by layer, and constructed a hydrogel construct carrying cells *in vivo* [170]. This provides a new method for clinical noninvasive surgery and a new direction for the application of photopolymerized hydrogels. At the same time, the photopolymerized hydrogel can simulate the advantages of the complex structure of the microenvironment *in vivo*, making it more practical in the construction of *in vitro* models, so that it can better understand the mechanism of tumor and disease [171,172].

In the future, appropriate photopolymerization materials, stable and high cell viability photopolymerization methods, and advanced engineering technology will help to design more complex tissue structures, which will enable better application in tissue engineering and regenerative medicine treatment.

Declaration of competing interest

The authors report no declarations of interest.

Acknowledgments

This work was financially supported by the National Natural Science Fund for Distinguished Young Scholars (No. 31525009), the National Natural Science Foundation of China (Nos. 31930067, 31771096), the National Key Research and Development Program of China (No. 2017YFC1103502), and 1·3·5 Project for Disciplines of Excellence, West China Hospital, Sichuan University (No. ZYGD18002).

References

[1] B.V. Slaughter, S.S. Khurshid, O.Z. Fisher, A. Khademhosseini, N.A. Peppas, Adv. Mater. 21 (2009) 3307–3329.
[2] J.Y. Sun, X.H. Zhao, W.R.K. Illeperuma, et al., Nature 489 (2012) 133–136.
[3] D.Y. Ko, U.P. Shinde, B. Yeon, B. Jeong, Prog. Polym. Sci. 38 (2013) 672–701.
[4] T. Bai, K. Zhao, Z. Lu, et al., Chin. Chem. Lett. 32 (2021) 1051–1054.
[5] P. Nezhad-Mokhtari, M. Ghorbani, L. Roshangar, J. Soleimani Rad, Int. J. Biol. Macromol. 139 (2019) 760–772.
[6] J. Silva, P. Vanat, D. Marques-da-Silva, J.R. Rodrigues, R. Lagoa, Bioact. Mater. 5 (2020) 447–457.
[7] A. Oryan, A. Kamali, A. Moshiri, H. Baharvand, H. Daemi, Int. J. Biol. Macromol. 107 (2018) 678–688.
[8] M.E.R. Jones, P.B. Messersmith, Biomaterials 28 (2007) 5215–5224.
[9] J.J. Yoon, H.J. Chung, T.G. Park, J. Biomed. Mater. Res. A 83A (2007) 597–605.
[10] D.H. Kim, J.W. Seok, A. Sung, J. Chosun Nat. Sci. 10 (2017) 148–153.
[11] K. Gwon, I. Han, S. Lee, Y. Kim, D.N. Lee, ACS Appl. Mater. Interfaces 12 (2020) 20234–20242.
[12] M. Lu, Y. Liu, Y.C. Huang, C.J. Huang, W.B. Tsai, Carbohydr. Polym. 181 (2018) 668–674.
[13] T. Hu, X. Cui, M. Zhu, et al., Bioact. Mater. 5 (2020) 808–818.
[14] A.D. Rouillard, C.M. Berglund, J.Y. Lee, et al., Tissue Eng. Part C: Methods 17 (2010) 173–179.
[15] S.T. Zheng, H.H. Yin, Z.G. Ma, et al., Chin. Chem. Lett. 30 (2019) 707–709.
[16] H. Cao, X. Ma, S. Sun, H. Su, T. Tan, Polym. Bull. 64 (2010) 623–632.
[17] K.Q. Huang, J. Wu, Z.P. Gu, ACS Appl. Mater. Interfaces 11 (2019) 2908–2916.
[18] G. Zhong, J. Yao, X. Huang, et al., Bioact. Mater. 5 (2020) 871–879.
[19] J. Huang, Y. Jiang, Y. Liu, et al., Bioact. Mater. 6 (2021) 770–782.
[20] J.A. Wieland, T.L. Houchin-Ray, L.D. Shea, J. Control. Release 120 (2007) 233–241.
[21] M. He, C.C. Chu, J. Appl. Polym. Sci. 130 (2013) 3736–3745.
[22] A.C. Borges, P.E. Bourban, D.P. Pioletti, J.A.E. Månson, Compos. Sci. Technol. 70 (2010) 1847–1853.
[23] X.H. Hu, C.Y. Gao, J. Appl. Polym. Sci. 110 (2008) 1059–1067.
[24] P.F. Chen, C. Xia, S. Mei, et al., Biomaterials 81 (2016) 1–13.
[25] M. Monier, Y. Wei, A.A. Sarhan, D.M. Ayad, Polymer 51 (2010) 1002–1009.
[26] X.Q. Deng, N.N. Chao, W. Ding, et al., J. Biomed. Nanotechnol. 15 (2019) 756–768.

[27] J. Lalevée, M.A. Tehfe, F. Dumur, et al., Macromol. Rapid Commun. 34 (2013) 239–245.
[28] K.S. Lim, J.H. Galarraga, X. Cui, et al., Chem. Rev. 120 (2020) 10662–10694.
[29] K.S. Lim, B.S. Schon, N.V. Mekhileri, et al., ACS Biomater. Sci. Eng. 2 (2016) 1752–1762.
[30] K. Dietliker, R. Hüsler, J.L. Birbaum, et al., Prog. Org. Coat. 58 (2007) 146–157.
[31] L. Tytgat, L. Van Damme, J. Van Hoorick, et al., Acta Biomater. 94 (2019) 340–350.
[32] C.M. Elvin, T. Vuocolo, A.G. Brownlee, et al., Biomaterials 31 (2010) 8323–8331.
[33] G. John, M. Morita, Macromolecules 32 (1999) 1853–1858.
[34] J.Y. Zhou, X. Allonas, A. Ibrahim, X.X. Liu, Prog. Polym. Sci. 99 (2019) 16.
[35] A. Szekely, M. Klussmann, Chem. Asian J. 14 (2019) 105–115.
[36] M. Abdallah, A. Hijazi, B. Graff, et al., Polym. Chem. 10 (2019) 872–884.
[37] J. Zhang, N. Hill, J. Lalevee, et al., Macromol. Rapid Commun. 39 (2018) 6.
[38] A. Eibel, D.E. Fast, G. Gescheidt, Polym. Chem. 9 (2018) 5107–5115.
[39] G. Ullrich, P. Burtscher, U. Salz, N. Moszner, R. Liska, J. Polym. Sci. Pol. Chem. 44 (2006) 115–125.
[40] X.H. Qin, A. Ovsianikov, J. Stampfl, R. Liska, Bio Nanomater. 15 (2014) 49–70.
[41] S.J. Bryant, C.R. Nuttelman, K.S. Anseth, J. Biomater. Sci. Polym. Ed. 11 (2000) 439–457.
[42] B.K. Mann, A.S. Gobin, A.T. Tsai, R.H. Schmedlen, J.L. West, Biomaterials 22 (2001) 3045–3051.
[43] L.H. Kang, P.A. Armstrong, L.J. Lee, et al., Ann. Biomed. Eng. 45 (2017) 360–377.
[44] T. Zhang, H. Chen, Y. Zhang, et al., Colloid Surf. B-Biointerfaces 174 (2019) 528–535.
[45] T. Billiet, E. Gevaert, T. De Schryver, M. Cornelissen, P. Dubruel, Biomaterials 35 (2014) 49–62.
[46] C.G. Williams, A.N. Malik, T.K. Kim, P.N. Manson, J.H. Elisseeff, Biomaterials 26 (2005) 1211–1218.
[47] N.E. Fedorovich, M.H. Oudshoorn, D. van Geemen, et al., Biomaterials 30 (2009) 344–353.
[48] C.S. Bahney, T.J. Lujan, C.W. Hsu, et al., Eur. Cells Mater. 22 (2011) 43–55.
[49] D.Y. Wong, T. Ranganath, A.M. Kasko, PLoS One 10 (2015) e0139307.
[50] D.E. Godar, C. Gurunathan, I. Ilev, Photochem. Photobiol. 95 (2019) 581–586.
[51] C. Lee, C.D. O'Connell, C. Onofrillo, et al., Stem Cells Transl. Med. 9 (2020) 302–315.
[52] Z.J. Wang, X. Jin, Z.L. Tian, et al., Adv. Healthc. Mater. 7 (2018) 11.
[53] P. Occhetta, R. Visone, L. Russo, et al., J. Biomed. Mater. Res. Part A 103 (2015) 2109–2117.
[54] C.H. Lin, K.F. Lin, K. Mar, S.Y. Lee, Y.M. Lin, Tissue Eng. Part C: Methods 22 (2016) 792–800.
[55] P. Occhetta, N. Sadr, F. Piraino, et al., Biofabrication 5 (2013) 035002.
[56] T. Majima, W. Schnabel, W. Weber, Die Makromol. Chem. 192 (1991) 2307–2315.
[57] B.D. Fairbanks, M.P. Schwartz, C.N. Bowman, K.S. Anseth, Biomaterials 30 (2009) 6702–6707.
[58] J. Konasch, A. Riess, M. Teske, et al., Curr. Dir. Biomed. Eng. 4 (2018) 141–144.
[59] N. Monteiro, W. He, C.M. Franca, A. Athirasala, L.E. Bertassoni, ACS Biomater. Sci. Eng. 4 (2018) 2563–2570.
[60] E.A. Kamoun, A. Winkel, M. Eisenburger, H. Menzel, Arab. J. Chem. 9 (2016) 745–754.
[61] J.A. Werkmeister, R. Adhikari, J.F. White, et al., Acta Biomater. 6 (2010) 3471–3481.
[62] A. Hoshikawa, Y. Nakayama, T. Matsuda, et al., Tissue Eng. 12 (2006) 2333–2341.
[63] M.H. Shahriari, M.A. Shokrgozar, S. Bonakdar, et al., Bull. Mat. Sci. 42 (2019) 7.
[64] Z. Wang, R. Abdulla, B. Parker, et al., Biofabrication 7 (2015) 045009.
[65] J. Hu, Y. Hou, H. Park, et al., Acta Biomater. 8 (2012) 1730–1738.
[66] T. Mazaki, Y. Shiozaki, K. Yamane, et al., Sci. Rep. 4 (2014) 4457.
[67] M. Khanmohammadi, S. Nemati, J. Ai, F. Khademi, Mater. Sci. Eng. C: Mater. Biol. Appl. 103 (2019) 9.
[68] K.S. Lim, B.J. Klotz, G.C.J. Lindberg, et al., Macromol. Biosci. 19 (2019) 1900098.
[69] Y.H. Niu, T. Yang, R.Y. Ke, C. Wang, Mater. Express 9 (2019) 563–569.
[70] Y.J. Xu, X. Wu, S.Y. Wang, et al., J. Biomed. Nanotechnol. 15 (2019) 2351–2362.
[71] X. He, B. Zhu, W. Xie, et al., Bioact. Mater. 6 (2021) 299–311.
[72] L. Moller, A. Krause, J. Dahlmann, et al., Int. J. Artif. Organs 34 (2011) 93–102.
[73] L.A. Wells, M.A. Brook, H. Sheardown, Generic, Macromol. Biosci. 11 (2011) 988–998.
[74] C. Qi, J. Liu, Y. Jin, et al., Biomaterials 163 (2018) 89–104.
[75] J. Wang, X. Wang, M. Li, S. Fan, Mater. Express 10 (2020) 1116–1121.
[76] Y.C. Chen, R.Z. Lin, H. Qi, et al., Adv. Funct. Mater. 22 (2012) 2027–2039.
[77] H. Shin, B.D. Olsen, A. Khademhosseini, Biomaterials 33 (2012) 3143–3152.
[78] T.H. Barker, Biomaterials 32 (2011) 4211–4214.
[79] D. Jhala, H. Rather, D. Kedaria, et al., Bioact. Mater. 4 (2019) 79–86.
[80] Luo, S.Y. Zhu, Y. Li, et al., J. Biomed. Nanotechnol. 16 (2020) 842–852.
[81] Q. Liu, H. Wang, G. Li, et al., Chin. Chem. Lett. 30 (2019) 485–488.
[82] Y.L. Li, J. Rodrigues, H. Tomas, Chem. Soc. Rev. 41 (2012) 2193–2221.
[83] S. Bertlein, G. Brown, K.S. Lim, et al., Adv. Mater. 29 (2017) 1703404.
[84] E. Ohuchi, K. Imai, Y. Fujii, et al., J. Biol. Chem. 272 (1997) 2446–2451.
[85] X.P. Xu, Z.H. Chen, Y. Wang, L. Bonewald, B. Steffensen, Biochem. J. 406 (2007) 147–155.
[86] K. Yue, G.T.D. Santiago, M.M. Alvarez, et al., Biomaterials 73 (2015) 254–271.
[87] X.H. Qin, J. Torgersen, R. Saf, et al., J. Polym. Sci. Pol. Chem. 51 (2013) 4799–4810.
[88] M. Susec, R. Liska, G. Russmuller, J. Kotek, P. Krajnc, Macromol. Biosci. 15 (2015) 253–261.
[89] H.P. Tan, C.R. Chu, K.A. Payne, K.G. Marra, Biomaterials 30 (2009) 2499–2506.
[90] C.B. Highley, G.D. Prestwich, J.A. Burdick, Curr. Opin. Biotechnol. 40 (2016) 35–40.
[91] L. Ouyang, C.B. Highley, C.B. Rodell, W. Sun, J.A. Burdick, ACS Biomater. Sci. Eng. 2 (2016) 1743–1751.
[92] X. Jia, J.A. Burdick, J. Kobler, et al., Macromolecules 37 (2004) 3239–3248.
[93] X.H. Qin, P. Gruber, M. Markovic, et al., Polym. Chem. 5 (2014) 6523–6533.
[94] C. Vepari, D.L. Kaplan, Prog. Polym. Sci. 32 (2007) 991–1007.
[95] B. Kundu, R. Rajkhowa, S.C. Kundu, X.G. Wang, Adv. Drug Deliv. Rev. 65 (2013) 457–470.
[96] X. Cui, B.G. Soliman, C.R. Alcala-Orozco, et al., Adv. Healthc. Mater. 9 (2020) 1901667.
[97] S.H. Kim, Y.K. Yeon, J.M. Lee, et al., Nat. Commun. 9 (2018) 1620.
[98] Y. Zhou, K. Liang, S. Zhao, et al., Int. J. Biol. Macromol. 108 (2018) 383–390.
[99] J.L. Whittaker, N.K. Dutta, C.M. Elvin, N.R. Choudhury, J. Mat. Chem. B 3 (2015) 6576–6579.
[100] A. Sun, X.Y. He, L. Li, et al., NPG Asia Mater. 12 (2020) 11.
[101] M. Ishihara, Trends Glycosci. Glycotechnol. 14 (2002) 331–341.
[102] J.W. Bjork, S.L. Johnson, R.T. Tranquillo, Biomaterials 32 (2011) 2479–2488.
[103] K. Holzl, S.M. Lin, L. Tytgat, et al., Biofabrication 8 (2016) 19.
[104] J.L. Ifkovits, J.A. Burdick, Tissue Eng. 13 (2007) 2369–2385.
[105] J.F. Liu, J. Wang, Q.Q. Zhu, et al., J. Biomed. Nanotechnol. 15 (2019) 1454–1467.
[106] T. Serra, M. Ortiz-Hernandez, E. Engel, J.A. Planell, M. Navarro, Mater. Sci. Eng. C: Mater. Biol. Appl. 38 (2014) 55–62.
[107] Y.F. Ma, W.J. Zhang, Z.H. Wang, et al., Acta Biomater. 44 (2016) 110–124.
[108] L. Bedouet, F. Pascale, L. Moine, et al., Int. J. Pharm. 456 (2013) 536–544.
[109] X. Wang, C.P. Wang, X.Y. Wang, et al., Chem. Mat. 29 (2017) 1370–1376.
[110] L.M. Weber, C.G. Lopez, K.S. Anseth, J. Biomed. Mater. Res. A 90A (2009) 720–729.
[111] A.S. Sawhney, C.P. Pathak, J.A. Hubbell, Macromolecules 26 (1993) 581–587.
[112] A. Mautner, X.H. Qin, H. Wutzel, et al., J. Polym. Sci. Pol. Chem. 51 (2013) 203–212.
[113] L. Moradi, M. Vasei, M.M. Dehghan, et al., Biomaterials 126 (2017) 18–30.
[114] C. Zhang, K. Liang, D. Zhou, et al., ACS Appl. Mater. Interfaces 10 (2018) 27692–27700.
[115] K.S. Lim, R. Levato, P.F. Costa, et al., Biofabrication 10 (2018) 034101.
[116] B. Li, Y.L. Gao, L.K. Guo, et al., Regen. Biomater. 5 (2018) 159–166.
[117] Y. Zamani, M. Rabiee, M.A. Shokrgozar, S. Bonakdar, M. Tahriri, Appl. Biochem. Biotechnol. 171 (2013) 1513–1524.
[118] S.H. Cho, S.M. Lim, D.K. Han, et al., J. Biomater. Sci. Polym. Ed. 20 (2009) 863–876.
[119] E. Tziampazis, J. Kohn, P.V. Moghe, Biomaterials 21 (2000) 511–520.
[120] Y.X. Dong, A. Sigen, M. Rodrigues, et al., Adv. Funct. Mater. 27 (2017) 12.
[121] M.T. Spang, K.L. Christman, Acta Biomater. 68 (2018) 1–14.
[122] S.X. Lu, K.S. Anseth, Macromolecules 33 (2000) 2509–2515.
[123] I.T. Ozbolat, M. Hospodiuk, Biomaterials 76 (2016) 321–343.
[124] T. Billiet, M. Vandenhaute, J. Schelfhout, S. Van Vlierberghe, P. Dubruel, Biomaterials 33 (2012) 6020–6041.
[125] J.Z. Manapat, Q.Y. Chen, P. Ye, R.C. Advincula, Macromol. Mater. Eng. 302 (2017) 13.
[126] H. Fukumoto, S. Nagano, N. Kawatsuki, T. Seki, Chem. Mat. 18 (2006) 1226–1234.
[127] N. Annabi, A. Tamayol, J.A. Uquillas, et al., Adv. Mater. 26 (2014) 85–124.
[128] Y.Z. Zhu, J. Shen, L. Yin, et al., Chem. Eng. J. 366 (2019) 112–122.
[129] V.L. Tsang, A.A. Chen, L.M. Cho, et al., FASEB J. 21 (2007) 790–801.
[130] P. Zorlutuna, N. Annabi, G. Camci-Unal, et al., Adv. Mater. 24 (2012) 1782–1804.
[131] F.P.W. Melchels, J. Feijen, D.W. Grijpma, Biomaterials 31 (2010) 6121–6130.
[132] L. Elomaa, E. Keshi, I.M. Sauer, M. Weinhart, Mater. Sci. Eng. C 112 (2020) 110958.
[133] P. Chen, L. Zheng, Y. Wang, et al., Theranostics 9 (2019) 2439–2459.
[134] R. Raman, R. Bashir, Stereolithographic 3D bioprinting for biomedical applications, in: A. Atala, J.J. Yoo (Eds.), Essentials of 3D Biofabrication and Translation, Academic Press, Boston, 2015, pp. 89–121.
[135] A. de Leon, Q.Y. Chen, N.B. Palaganas, et al., React. Funct. Polym. 103 (2016) 141–155.
[136] H. Hong, Y.B. Seo, D.Y. Kim, et al., Biomaterials 232 (2020) 119679.
[137] J. Hong, Y. Shin, S. Kim, J. Lee, C. Cha, Adv. Funct. Mater. 29 (2019) 1808750.
[138] B.K. Sun, Z. Siprashvili, P.A. Khavari, Science 346 (2014) 941.
[139] R.A. Kamel, J.F. Ong, E. Eriksson, J.P.E. Junker, E.J. Caterson, J. Am. Coll. Surg. 217 (2013) 533–555.
[140] G.C. Gurtner, S. Werner, Y. Barrandon, M.T. Longaker, Nature 453 (2008) 314–321.
[141] F. Groeber, M. Holeiter, M. Hampel, S. Hinderer, K. Schenke-Layland, Adv. Drug Deliv. Rev. 63 (2011) 352–366.
[142] I.C. Carvalho, H.S. Mansur, Mater. Sci. Eng. C: Mater. Biol. Appl. 78 (2017) 690–705.
[143] G. Eke, N. Mangir, N. Hasirci, S. MacNeil, V. Hasirci, Biomaterials 129 (2017) 188–198.
[144] A. Skardal, S.V. Murphy, K. Crowell, et al., J. Biomed. Mater. Res. B 105 (2017) 1986–2000.
[145] T.R. Schneider, R. Hakami-Tafreshi, A. Tomasino-Perez, L. Tayebi, D. Lobner, Dent. Mater. J. 38 (2019) 579–583.
[146] I. Sideridou, V. Tserki, G. Papanastasiou, Biomaterials 23 (2002) 1819–1829.

[147] N.J. Walters, W.D. Xia, V. Salih, P.F. Ashley, A.M. Young, Dent. Mater. 32 (2016) 264–277.
[148] Q. Fu, H.J. Ren, C. Zheng, et al., J. Biomater. Appl. 33 (2018) 477–487.
[149] J. Huang, Z. Wang, S. Krishna, et al., Mater. Express 10 (2020) 975–985.
[150] M. Alipour, M. Aghazadeh, A. Akbarzadeh, et al., Artif. Cell. Nanomed. Biotechnol. 47 (2019) 3431–3437.
[151] N. Monteiro, G. Thrivikraman, A. Athirasala, et al., Dent. Mater. 34 (2018) 389–399.
[152] C. Fukaya, A. Ishikawa, Y. Nakayama, et al., J. Photochem. Photobiol. A: Chem. 199 (2008) 255–260.
[153] M.S. Bae, J.E. Kim, J.B. Lee, et al., Carbohydr. Polym. 92 (2013) 167–175.
[154] Y. Huang, H. Li, X. He, et al., Chin. Chem. Lett. 31 (2020) 787–791.
[155] H. Qu, H. Fu, Z. Han, Y. Sun, RSC Adv. 9 (2019) 26252–26262.
[156] X. Zhai, C. Ruan, Y. Ma, et al., Adv. Sci. 5 (2018) 1700550.
[157] G. Cidonio, C.R. Alcala-Orozco, K.S. Lim, et al., Biofabrication 11 (2019) 035027.
[158] M. Kesti, M. Muller, J. Becher, et al., Acta Biomater. 11 (2015) 162–172.
[159] J. Shao, Z. Ding, L. Li, et al., J. Photochem. Photobiol. B:Biol. 203 (2020) 111744.
[160] H. Lin, A.W.M. Cheng, P.G. Alexander, A.M. Beck, R.S. Tuan, Tissue Eng. A 20 (2014) 2402–2411.
[161] K.S. Lim, M. Baptista, S. Moon, T.B.F. Woodfield, J. Rnjak-Kovacina, Trends Biotechnol. 37 (2019) 1189–1201.
[162] G. Camci-Unal, N. Annabi, M.R. Dokmeci, R. Liao, NPG Asia Mater. 6 (2014) 12.
[163] Z.Q. Li, J.J. Guan, Polymers 3 (2011) 740–761.
[164] S. Anil Kumar, M. Alonzo, S.C. Allen, et al., ACS Biomater. Sci. Eng. 5 (2019) 4551–4563.
[165] M. Izadifar, D. Chapman, P. Babyn, X. Chen, M.E. Kelly, Tissue Eng. Part C: Methods 24 (2017) 74–88.
[166] R.Z. Lin, Y.C. Chen, R. Moreno-Luna, A. Khademhosseini, J.M. Melero-Martin, Biomaterials 34 (2013) 6785–6796.
[167] W. Liu, Y.S. Zhang, M.A. Heinrich, et al., Adv. Mater. 29 (2017) 1604630.
[168] J.A. Burdick, W.L. Murphy, Nat. Commun. 3 (2012) 1269.
[169] J.W. Seo, S.R. Shin, Y.J. Park, H. Bae, Tissue Eng. Regen. Med. 17 (2020) 423–431.
[170] Y. Chen, J. Zhang, X. Liu, et al., Sci. Adv. 6 (2020) eaba7406.
[171] Y. Wang, W. Shi, M. Kuss, et al., ACS Biomater. Sci. Eng. 4 (2018) 4401–4411.
[172] E. Goulart, L.C. de Caires-Junior, K.A. Telles-Silva, et al., Biofabrication 12 (2019) 015010.